Injection and detection of ballistic electrical currents in silicon

Hui Zhao[1] and Arthur L. Smirl[2,a)]
[1]*Department of Physics and Astronomy, University of Kansas, Lawrence, Kansas 66045, USA*
[2]*Laboratory for Photonics and Quantum Electronics, University of Iowa, Iowa City, Iowa 52242, USA*

(Received 21 September 2010; accepted 2 November 2010; published online 24 November 2010)

Ballistic electrical currents are injected in Si at 80 K by the quantum interference between the indirect one-photon and two-photon absorptions of a pair of phase-locked harmonically related pulses. The average distance that the electrons and holes move (weighted by their respective free-carrier absorption cross sections) is detected using phase-dependent differential transmission techniques that have a sensitivity of $\sim 10^{-7}$, nanometer spatial, and 100 fs temporal resolutions. The indirect, phonon-assisted injection process is approximately 50 times weaker than in GaAs, and it causes a relative shift in electron and hole profiles that decays in ~ 100 fs, but it also results in a shift in the center of mass that persists until it is destroyed by diffusion and recombination on longer time scales. Movement of the electrons or holes of at least 0.4 nm is observed and confirms that the current is an injection, not a rectification, current. © *2010 American Institute of Physics*. [doi:10.1063/1.3518719]

The generation and control of ballistic currents and the detection of charge motion over nanometer dimensions (comparable to the mean free path) and on femtosecond time scales (comparable to the momentum relaxation time) in technologically relevant materials become increasingly important as semiconductor device features are reduced to the tens of nanometer regime. Recently, we have demonstrated that the combination of quantum interference for injection and control and of phase-sensitive differential transmission techniques for detection provides a promising platform for studying ballistic charge transport in GaAs.[1] While GaAs was chosen for initial demonstrations (because it is a direct band gap material, it is relatively well characterized, and it is the semiconductor most frequently used for photonic applications), Si is the most common choice for electronic applications. However, despite a recent revival of interest in Si for photonic applications,[2] historically, it has seldom been used as a photonic material, primarily because it is an indirect band gap semiconductor, exhibits inversion symmetry, and consequently, has a vanishing $\chi^{(2)}$, and therefore, interacts only weakly with light. Nevertheless, in this letter, we demonstrate that phase-sensitive detection can be used to monitor ballistic electrical currents generated in Si by quantum interference techniques.

The procedure that we use to inject ballistic electrical currents [or pure charge currents (PCCs)] into Si is similar to that described previously for GaAs (Refs. 1 and 3–9) and is shown in Fig. 1(a). An ~ 100 fs [full width at half maximum (FWHM) pulse ($\lambda = 1450$ nm, $\hbar\omega = 0.8566$ eV) is obtained from an optical parameter oscillator (OPO) pumped at 80 MHz by a Ti:sapphire laser, and a 2ω pulse is obtained by second harmonic generation in a beta barium borate (BBO) crystal. The phase difference $\Delta\phi = 2\phi_\omega - \phi_{2\omega}$ [where ϕ_ω ($\phi_{2\omega}$) is the phase of the ω (2ω) pulse] is controlled by a scanning dichroic interferometer. The two pulses copropagate along the z-direction (100 direction) and are focused to a diameter of ~ 2 μm (FWHM) in a 750-nm-thick silicon layer grown on a 350-μm-thick sapphire substrate cooled to 80 K. The fluences of the 2ω pulse (~ 64 μJ/cm^2) and ω pulse (~ 16 mJ/cm^2) are adjusted to produce the same peak carrier density of $\sim 5 \times 10^{17}$ cm^{-3}.

The energy $2\hbar\omega$ (1.713 eV) is below the direct band gap (3.4 eV), but above the indirect gap (1.17 eV) of Si, but $\hbar\omega$ is below both the direct and the indirect gaps [see Fig. 1(b)]. Therefore, the interference is between phonon-assisted *indirect* one-photon absorption of 2ω and phonon-assisted indirect two-photon absorption of ω. This is in contrast to our previous experiments in GaAs,[1,3–9] where $2\hbar\omega$ was above the direct gap and the interference was between *direct* one-photon and two-photon absorption pathways. However, like

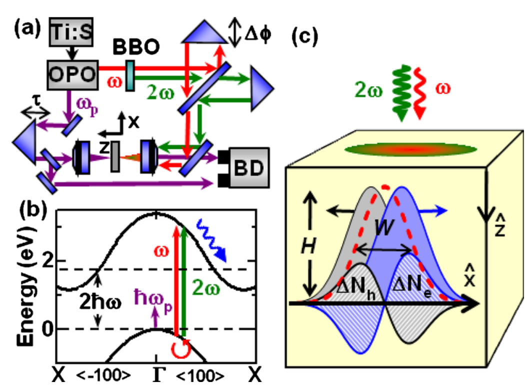

FIG. 1. (Color online) (a) Experimental apparatus for injecting and detecting ballistic electrical currents: Ti:S, OPO, BBO, and BD denote a mode-locked titanium sapphire laser, an optical parametric oscillator, a beta barium borate crystal, and a balanced detector, respectively. (b) The key features of the Si band structure, with the nonresonant quantum interference between the indirect two-photon absorption of the ω pulse and one-photon absorption of the 2ω pulse indicated by the longer arrows and with the probe (ω_p) shown as the shorter arrow. Phonon-assisted scattering is indicated by a wavy arrow. (c) Schematic showing the injection of charge current by co-linearly polarized (along x) ω and 2ω pulses. The electrons and holes are initially injected with identical Gaussian spatial density profiles (dashed curve of height H and width W). For $\Delta\phi = 3\pi/2$, the electrons (holes) move to the right (left) with average velocity $\langle v_e \rangle$ ($\langle v_h \rangle$). As a result, the electrons (holes) travel a distance x_e (x_h) in time t. The left (right) cross hatched area indicates the differential change in the electron density ΔN_e (hole density ΔN_h) caused by the carrier motion.

a)Electronic mail: art-smirl@uiowa.edu.

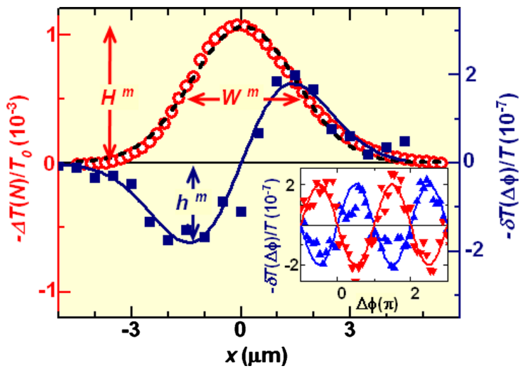

FIG. 2. (Color online) The Gaussian spatial profile of the phase-independent differential transmission, $\Delta T(N)/T_0$ (open circles), and the derivativelike spatial profile of the phase-dependent differential transmission, $\delta T(\Delta\phi)/T$ (solid squares), are shown as a function of position along the x-axis ($y=0$) for a fixed time delay of 5 ps and for fixed phases of $\Delta\phi=0$ and $\Delta\phi=\pi/2$, respectively. The measured height H^m and width W^m of the profile are extracted by fitting the $\Delta T(N)/T_0$ data to a Gaussian (dashed line), and h^m [the maximum $\delta T(\Delta\phi)/T$] by fitting the $\delta T(\Delta\phi)/T$ data to the derivative of that Gaussian (solid line). The inset shows the phase-dependent differential transmission $\delta T(\Delta\phi)/T$ as a function of phase for the same fixed time delay and for fixed positions of $x=+1.5$ (up-triangles) and -1.5 μm (down-triangles). The solid lines in the inset are cosinusoidal fits to the data.

the GaAs case, simultaneous absorption of ω and 2ω is expected (in the rigid shift approximation) to inject identical Gaussian profiles for the electrons and holes with oppositely directed average initial velocities $\langle v_e(t=0)\rangle \sin\Delta\phi$ and $\langle v_h(t=0)\rangle \sin\Delta\phi$, respectively. As momentum relaxation destroys the ballistic current, the electrons and holes continue to separate and to form a space-charge field, which opposes the separation and eventually causes the electrons and holes to return to a common position. If the relative spatial shift of the electron and hole profiles is small compared to the width of the original profile (W), then the net changes in the electron and hole densities will follow the derivative of the original profile [see Fig. 1(c)].

The spatial profile $N(\Delta\phi=0;x,y;t)$ of the electrons and holes in the absence of current generation is obtained by measuring the differential transmission $\Delta T(N;x,y,;t)/T_0 \equiv [T(\Delta\phi=0;x,y;t)-T_0]/T_0$ associated with the free-carrier absorption of a weak probe pulse ($\lambda=1760$ nm) taken from the idler of the OPO [where T is the transmission of the probe at position (x,y) on the sample surface at time t established by a carrier density N with the pumps present and T_0 is the linear transmission without the pumps]. $\Delta T(N)/T_0 = -[\sigma_e(t)+\sigma_h(t)]NL$, where $\sigma_{e(h)}$ is the free-carrier absorption cross section for the electrons (holes), in the limit in which $[\sigma_e(t)+\sigma_h(t)]NL \ll 1$. For measurements of $\Delta T(N)/T_0$, the pump beams are modulated with a mechanical chopper, and the probe transmission is detected using a lock-in tuned to the chopper frequency. A typical spatial profile of $\Delta T(N)/T_0$ measured by scanning the probe along the x-axis ($y=0$) for a fixed time delay of 5 ps is shown in Fig. 2. Using $\sigma_e(t)+\sigma_h(t)=1.5\times10^{-17}$ cm^2 (scaled from Ref. 10) and a peak carrier density of 10^{18} cm^{-3}, we estimate a peak $\Delta T(N)/T_0 \sim -10^{-3}$, in excellent agreement with the measured value. We have also separately verified[11] that $\Delta T(N)/T_0$ is proportional to N over the density range created here and that diffusion and recombination are negligible on the time scales of a few picoseconds. The measured height H^m and width W^m (FWHM) of the profile are indicated in Fig. 2.

The carrier transport is monitored by measuring the $\Delta\phi$-*dependent* differential transmission of the probe: $\delta T(\Delta\phi;x,y;t)/T \equiv [T(\Delta\phi;x,y;t)-T(0;x,y;t)]/T(0;x,y;t)$, i.e., by measuring the difference in transmission with and without current injection. An electro-optic modulator in one arm of the interferometer (not shown) dithers $\Delta\phi$ about its set value, and $\delta T(\Delta\phi;x,y;t)/T$ is measured by slaving the lock-in amplifier to the modulator. Again, for small absorbance changes, $\delta T(\Delta\phi)/T = -[\sigma_e(t)\Delta N_e(\Delta\phi)+\sigma_h(t)\Delta N_h(\Delta\phi)]L$, where $\Delta N_{e(h)}(\Delta\phi) \equiv N_{e(h)}(\Delta\phi)-N_{e(h)}(\Delta\phi=0)$ denotes the difference in the electron (hole) profiles with and without current injection. If the average distance moved per electron (hole), $x_{e(h)} \ll W$, then $\Delta N_{e(h)}(\Delta\phi) = -x_{e(h)}\partial N_{e(h)} \times(0)/\partial x$. For each fixed time delay, $\delta T/T$ versus $\Delta\phi$ is measured at each x ($y=0$) (as illustrated for $x=\pm1.5$ μm in the inset of Fig. 2). Subsequently, the peak $\delta T/T$ at $\Delta\phi=\pi/2$ (maximum current injection) is plotted as a function of x ($y=0$). Notice that $\delta T(\Delta\phi)/T$ varies sinusoidally with phase and exhibits a derivativelike spatial profile, thus providing convincing evidence of PCC injection in Si. Finally, the peak height of the derivative, h^m, is extracted, as illustrated in Fig. 2.

It is not surprising that PCC injection is weaker and that measuring the ballistic transport is more difficult in Si than in GaAs.[1] Specifically, at the densities used here, $\Delta T(N)/T_0$ is $\sim$500 times larger in GaAs than in Si. This is primarily because the probe interrogates the saturation of direct transitions in GaAs and free-carrier transitions in Si, and the "cross section" for the former is much larger than for the latter. By comparison, $\delta T(\Delta\phi)/T$ is $\sim 3\times10^4$ times larger in GaAs. This is, in part, due to the relative strengths of direct and free-carrier absorptions, as we have just discussed, but it is also a consequence of the weaker quantum interference process in Si, which is nonresonant (in the sense that $2\hbar\omega$ is not sufficient to *directly* couple states in the valence and conduction band) and indirect (in the sense that it requires phonon participation).

As we have discussed previously,[1] it is straightforward to extract a parameter $\langle x\rangle = [(\sigma_e x_e+\sigma_h x_h)/(\sigma_e+\sigma_h)] \cong 0.7h^m W^m/H^m$ from the measurements in Fig. 2. This parameter has units of distance and is the average distance moved by the electrons plus the holes weighted by the sensitivity of the probe to each species. The dynamics of $\langle x\rangle$ is obtained by repeating the procedure illustrated in Fig. 2 as a function of time delay; the results are shown in Fig. 3.

It is convenient to discuss the qualitative behavior of $\langle x\rangle$ (shown in Fig. 3) by assuming that the electron and hole profiles do not broaden or change shape during transport[1] and that the free-carrier cross sections scale inversely with the effective masses [i.e., $\sigma_e/\sigma_h = m_h^*/m_e^*$, where $m_{e(h)}^*$ is the effective mass of the electron (hole)]. In addition, if the conduction and valence bands of Si are initially assumed to be parabolic, then our previous results for a rigid shift yield[1]

$$\langle x\rangle = -\left(\frac{m_e^*-m_h^*}{m_e^*+m_h^*}\right)\frac{\langle v_R(0)\rangle\tau_m \sin(\Delta\phi)}{\sqrt{1-4(\Omega\tau_m)^2}}e^{-t/2\tau_m} \times\left[e^{-\sqrt{1-4(\Omega\tau_m)^2}(t/2\tau_m)} - e^{\sqrt{1-4(\Omega\tau_m)^2}(t/2\tau_m)}\right], \quad (1)$$

where Ω is the plasma frequency, τ_m is the momentum relaxation time, and $\langle v_R(0)\rangle = \langle v_e(0)\rangle - \langle v_h(0)\rangle$ is the relative initial average velocity when $\Delta\phi=\pi/2$. In writing this ex-

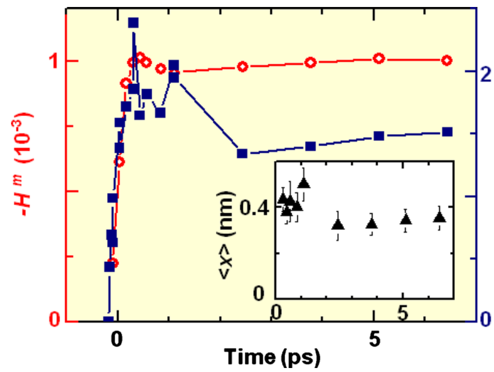

FIG. 3. (Color online) The peak phase-independent (open circles) and phase-dependent (solid squares) differential transmissions, $H^m(t)$ and $h^m(t)$, respectively, measured by repeating the procedure summarized in Fig. 2 as a function of time delay. The inset shows the net carrier transport length, $\langle x\rangle=[(\sigma_e x_e+\sigma_h x_h)/(\sigma_e+\sigma_h)]$, extracted from these quantities.

pression, we have assumed that the generation process is instantaneous and ignored (for the moment) the possibility of a displacement of the center of mass of the electron-hole distributions.

For our carrier densities, $\langle x\rangle$ is roughly critically damped ($\Omega\tau_m\sim 1/2$). Therefore, based on Eq. (1), we expect the electrons and holes (injected with oppositely directed velocities) to move apart, a space-charge field to form, and the carriers to return to their original positions in $\tau_m\sim 100$ fs. Such a picture is similar to the dynamics observed in GaAs (Ref. 1) and is also consistent with the recently observed subpicosecond decays of terahertz radiation emitted by charge currents injected into Si by quantum interference.[12,13] In contrast, here (Fig. 3), the electrons and holes move apart by $\sim$0.4 nm in $\sim$100 fs, and they do not return to their *original* positions on picosecond time scales.

At first, the behavior of $\langle x\rangle$ seems to be counterintuitive and to contradict the terahertz measurements.[12,13] However, this is because we have assumed parabolic bands. If the bands are parabolic, the hydrodynamic equations for the relative (x_e-x_h) and center-of-mass $[(m_e^* x_e+m_h^* x_h)/(m_e^*+m_h^*)]$ coordinates are decoupled, and there is no center-of-mass motion. If the bands are not parabolic, then the two coordinates are coupled and the center of mass is displaced. Consequently, we speculate that the carriers reach a *common* position (i.e., the relative motion and the space-charge field decay) in $\sim$100 fs, but this position is different from the original position (i.e., the center of mass has moved). Such behavior has been discussed previously in GaAs.[9] Notice that terahertz techniques[12,13] only detect (time-dependent) relative motion but are not sensitive to center-of-mass motion.

The parameter $\langle x\rangle$ is $\sim$50 times larger in GaAs than in Si partly because of the weaker nature of the quantum interference process in Si but also because $\langle x\rangle$ is a weighted average of electron and hole motion. This can be seen by remembering that in both materials, the electrons and the holes are injected with oppositely directed initial velocities; therefore, as depicted in Fig. 1, x_e and x_h initially have opposite signs. In our previous experiments in GaAs,[1,5,7,8] the probe was primarily sensitive to the electrons ($\sigma_e>\sigma_h$), in which case $\langle x\rangle$ corresponds to x_e. In Si, the effective masses of the heavy hole and indirect valleys are comparable; therefore, one might expect $\sigma_e\sim\sigma_h$. In this case, the oppositely directed hole motion tends to subtract from the electron movement in determining $\langle x\rangle$. In fact, if the probe were equally sensitive to electrons and holes ($\sigma_e=\sigma_h$) and if they were to move the same distance in opposite directions (i.e., $x_e=-x_h$), $\langle x\rangle=0$. This weighting and cancellation associated with the electron and hole contributions to the probe differential transmission is another difference between this technique and the terahertz technique.[12,13] In some cases, this feature makes it easier to separate and analyze the electron [e.g., GaAs (Ref. 1)] and hole [e.g., Ge (Ref. 14)] dynamics. Here, it results in a slightly weaker signal and complicates the interpretation. Nevertheless, from Fig. 3, it is clear that the carriers move (either relative or center-of-mass motion) by at least 0.4 nm. While both the optical rectification currents and the injection of electrical currents are allowed for the experimental geometries used in Refs. 12 and 13 and are used here, this average distance shows conclusively that charge is injected and that it moves macroscopic distances—inconsistent with optical rectification.

In summary, we have demonstrated that a platform consisting of quantum interference for injection and phase-sensitive spatially resolved pump-probe techniques for detection can be used to study ballistic charge transport in Si. We have shown that quantum interference between one-photon and two-photon absorptions of two phase-related pulses can be used to inject ballistic electrical (or charge) currents into Si even though the process is phonon-assisted and nonresonant. As in GaAs, these quantum interference techniques are noninvasive, and they allow the phase and polarization of the pump pulses to be used to precisely control the amplitude, sign, and direction of the injected currents.

We acknowledge insightful discussions with Henry van Driel, Markus Betz, and John Sipe. This work was supported in part by NSF, ONR, and DARPA.

[1] H. Zhao, E. J. Loren, A. L. Smirl, and H. M. van Driel, J. Appl. Phys. **103**, 053510 (2008).
[2] L. Pavesi and D. J. Lockwood, *Silicon Photonics* (Springer, New York, 2004).
[3] R. Atanasov, A. Haché, J. L. P. Hughes, H. M. van Driel, and J. E. Sipe, Phys. Rev. Lett. **76**, 1703 (1996).
[4] A. Haché, Y. Kostoulas, R. Atanasov, J. L. P. Hughes, J. E. Sipe, and H. M. van Driel, Phys. Rev. Lett. **78**, 306 (1997).
[5] M. J. Stevens, A. Najmaie, R. D. R. Bhat, J. E. Sipe, H. M. van Driel, and A. L. Smirl, J. Appl. Phys. **94**, 4999 (2003).
[6] T. M. Fortier, P. A. Roos, D. J. Jones, S. T. Cundiff, R. D. R. Bhat, and J. E. Sipe, Phys. Rev. Lett. **92**, 147403 (2004).
[7] M. J. Stevens, R. D. R. Bhat, X. Y. Pan, H. M. van Driel, J. E. Sipe, and A. L. Smirl, J. Appl. Phys. **97**, 093709 (2005).
[8] H. Zhao, E. J. Loren, H. M. van Driel, and A. L. Smirl, Phys. Rev. Lett. **96**, 246601 (2006).
[9] Y. Kerachian, P. A. Marsden, H. M. van Driel, and A. L. Smirl, Phys. Rev. B **75**, 125205 (2007).
[10] T. F. Boggess, K. M. Bohnert, K. Mansour, S. C. Moss, I. W. Boyd, and A. L. Smirl, IEEE J. Quantum Electron. **22**, 360 (1986).
[11] H. Zhao, Appl. Phys. Lett. **92**, 112104 (2008).
[12] L. Costa, M. Betz, M. Spasenović, A. D. Bristow, and H. M. van Driel, Nat. Phys. **3**, 632 (2007).
[13] M. Spasenović, M. Betz, L. Costa, and H. M. van Driel, Phys. Rev. B **77**, 085201 (2008).
[14] E. J. Loren, H. Zhao, and A. L. Smirl, J. Appl. Phys. **108**, 083111 (2010).